Available online at www.sciencedirect.com
ScienceDirect
Physics of the Earth and Planetary Interiors 158 (2006) 226–239
PHYSICS OF THE EARTH AND PLANETARY INTERIORS
www.elsevier.com/locate/pepi

Electrical anisotropy of South African lithosphere compared with seismic anisotropy from shear-wave splitting analyses

Mark P. Hamilton [a,b,*], Alan G. Jones [a], Rob. L. Evans [c], Shane Evans [d], C.J.S. Fourie [e], Xavier Garcia [a], Andy Mountford [f], Jessica E. Spratt [a], the SAMTEX MT Team [1]

[a] *Dublin Institute for Advanced Studies, 5 Merrion Square, Dublin 2, Ireland*
[b] *University of the Witwatersrand, School of Geosciences, Private Bag 3, Johannesburg, South Africa*
[c] *Woods Hole Oceanographic Institution, Department of Geology and Geophysics, Clark South 172, 360 Woods Hole Road, Woods Hole, MA 02543-1542, USA*
[d] *De Beers Group Services, Private Bag X01, Southdale 2135, South Africa*
[e] *Council for Geoscience, 280 Pretoria Street, Silverton, Pretoria, South Africa*
[f] *Rio Tinto Mineral Exploration Inc., P.O. Box 695, 7th Floor Castlemead, Lower Castle Street, Bristol BS99 1FS, UK*

Received 15 August 2005; received in revised form 15 December 2005; accepted 7 March 2006

Abstract

Electrical anisotropy in southern Africa, inferred from the analysis of magnetotelluric (MT) data recorded as part of the Southern African MT Experiment (SAMTEX), is compared with seismic anisotropy inferred from an SKS shear-wave splitting study in the same region. Given the vastly varying penetration depths in the survey area, electrical anisotropy is derived in terms of approximate depth, rather than frequency. Electrical anisotropy directions for crustal depths (<35 km) show more distinct variability than those for upper mantle depths, and, not surprisingly, appear to be strongly related to large-scale geological structures. Our results for upper lithospheric mantle depths (>45 km) are not consistent with the fast-axis directions inferred from the SKS analyses. Upper mantle electrical results appear to be mostly a consequence of the geometry of large-scale geological structures and provide evidence that some crustal structures are distinct at depth, while others seem to be confined to the crust. Our results indicate that the causative region for the seismic anisotropy in the lithospheric mantle has either a correspondingly weak electrical anisotropic signature, or is more prominent at greater lithospheric depths than those we investigate here.

Keywords: Anisotropy; Magnetotellurics; Geoelectric strike; Shear-wave splitting; Southern Africa

1. Introduction

The Kaapvaal craton in southern Africa is one of the most extensively studied Archean cratons in the world, largely due to the vast economic resources of the region (principally diamonds and gold), yet the formation mechanism, structure, and evolution of the craton and its surrounding terranes have still not been con-

* Corresponding author. Fax: +353 1 6621477.
E-mail address: mh@cp.dias.ie (M.P. Hamilton).

[1] Other members of the SAMTEX team are: Louise Collins, Clare Horan, Gerry Wallace, Dublin Institute for Advanced Studies; Alan Chave, Woods Hole Oceanographic Institution; Marisa Adlem, Kobus Raath, Edgar Stettler, Raimund Stettler, Council for Geoscience; Mark Muller, Sue Webb, University of the Witwatersrand.

0031-9201/$ – see front matter
doi:10.1016/j.pepi.2006.03.027

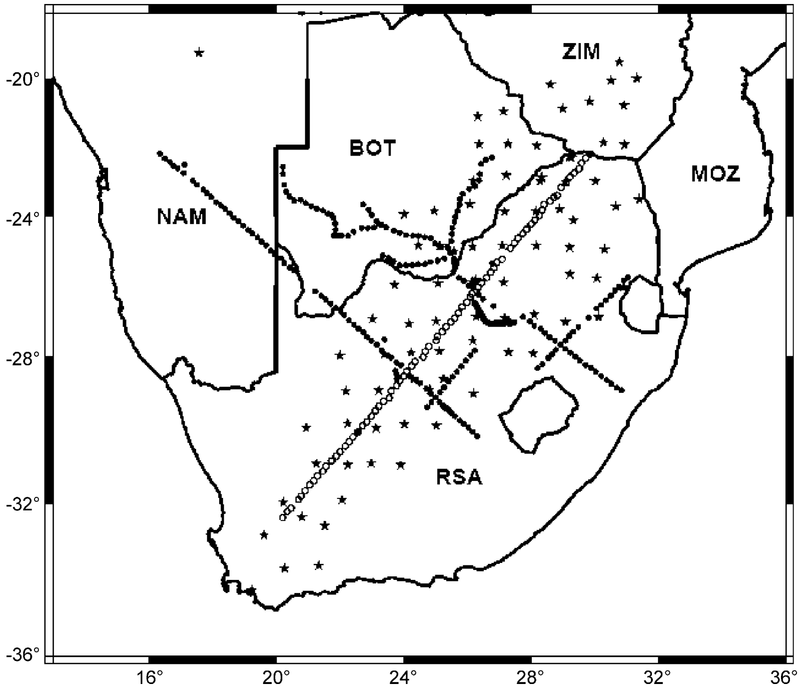

Fig. 1. Southern Africa with the Southern African Seismic Experiment (SASE) station locations represented by stars and the Southern African Magnetotelluric Experiment (SAMTEX) station locations from phases I and II represented as circles. Open circles denote the SAMTEX profile discussed in this paper. BOT: Botswana. MOZ: Mozambique. NAM: Namibia. RSA: Republic of South Africa. ZIM: Zimbabwe.

clusively resolved; basic, fundamental questions remain unanswered. The Southern African Seismic Experiment (SASE), part of the Kaapvaal Craton Project (Carlson et al., 1996, 2000), was conducted in southern Africa from 1997 to 1999 (Fig. 1), with the aim of investigating the seismic structure of the region. Broadband seismic stations were deployed on the Kaapvaal craton, part of the Zimbabwe craton, and on the surrounding mobile belts, and the results have been widely reported (Carlson et al., 2000; James et al., 2001; James and Fouch, 2002; Silver et al., 2001, 2004).

Initiated in 2003, the Southern African Magnetotelluric (MT) Experiment (SAMTEX) is being conducted by a consortium comprising academic, industry and government partners representing five countries from around the world (South Africa, Botswana, Namibia, Ireland and the USA). When completed, it will be the most extensive land-based MT study yet performed, and to date includes the collection of MT sounding data with broadband (~0.002 s to ~6000 s) magnetotelluric (BBMT) instruments at more than 330 sites (Fig. 1), and long period (20 s to ~10,000 s) magnetotelluric (LMT) instruments at approximately one-third of the BBMT sites to enhance depth penetration. The total length of the profiles is well over 5000 km, with BBMT stations spaced at nominally 20 km separation, and LMT stations spaced at 60 km (every third BBMT site), over a wide variety of geological terranes (Fig. 2).

The survey is being conducted in order to gain insight into the electrical structure of the crust and lithospheric mantle beneath the cratons of southern Africa, and their surrounding terranes, and, from that knowledge, to infer Archean and Proterozoic processes of formation and deformation. Unfortunately, due to logistical and security concerns we have been unable to extend the MT data acquisition into Zimbabwe, as originally planned, for complete comparison with the SASE results, and have instead expanded the experiment northwest into Namibia and Botswana and to the southeast of the main acquisition corridor (Fig. 1). As is the experience from other cratonic studies (e.g., the Slave craton in northern Canada, Davis et al., 2003, where electromagnetic, geochemical, and seismic results combined to give new insight into the understanding of the upper mantle of the region), it is expected that the combined results of SASE and SAMTEX, taken together with the superb geochemical and geological information, will complement each other and add considerably to our inferences of the tectonic history of southern Africa, and thereby to our understanding of Archean tectonic processes.

One important component of the SASE data analyses was the shear-wave splitting study conducted by

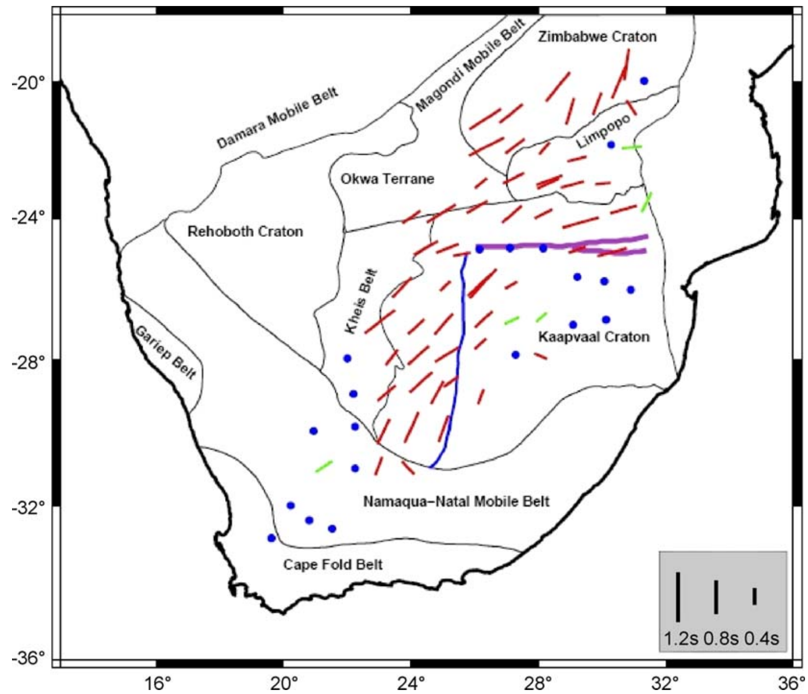

Fig. 2. Results from the shear-wave splitting measurements (fast polarisation directions) made by Silver et al. (2001), overlying a tectonic outline. High quality data are plotted in red, low quality in green, and stations with undetectable splitting in blue. Thabazimbi-Murchison Lineament (TML), as plotted by Silver et al. (2001), is represented as purple lines. Blue line: the N–S trending Colesburg Magnetic Lineament (CML). (For interpretation of the references to colour in this figure legend, the reader is referred to the web version of the article.)

Silver et al. (2001), further discussed by Silver et al. (2004). Derived SKS seismic anisotropy shows clear differences in splitting parameters over the various cratons and terranes, and was inferred to result from fossil anisotropy in the lithospheric mantle. In this paper we present electrical anisotropy results determined for the same region, compare them with the seismic anisotropy results of Silver et al. (2001, 2004), and consider what further insights may be obtained using this facet of the MT method.

2. Geological setting

The Archean Kaapvaal craton as a whole is composed of various granite-greenstone terrains, and is bounded to the south and west by Proterozoic mobile belts (Namaqua-Natal mobile belt and the Kheis belt), to the east by the Lebombo monocline (Jurassic in age), and to the north by the Neoarchean Limpopo mobile belt (de Wit et al., 1992). At its surface, the Kaapvaal craton can be divided into Archean subdomains (de Wit et al., 1992), and it has been suggested that some of these subdomains are also distinct at upper mantle depths within the deep lithospheric keel, or “tectosphere” (Jordan, 1975), typically found beneath Archean cratons. In the SASE data the Kaapvaal cratonic keel is in the form of a high velocity mantle zone observed by James et al. (2001) through tomographic analyses of P-wave and S-wave delay times. The eastern part of the craton is host to the oldest known sections (∼3.5 Gyr), some of which may represent the remnants of ancient oceanic lithosphere, whereas the more western sections of the craton are generally younger in age (de Wit et al., 1992). In contrast to the general ENE-WSW trend in the east of the craton, the western section of the Kaapvaal craton, to the west of the Colesburg Magnetic lineament (CML, Fig. 2) shows a distinctively N–S trend both geologically and geophysically, e.g., the Amalia and Kraaipan greenstone belts as well as the CML itself (Corner et al., 1990; de Wit et al., 1992).

The Limpopo belt (late Archean in age), separates the Kaapvaal and Zimbabwe cratons (Fig. 2), and can be divided into three different zones; the northern marginal zone, central zone, and southern marginal zone (de Wit et al., 1992). There is a large system of roughly ENE-WSW trending ductile shear zones that accommodated crustal shortening during the Limpopo Orogeny (McCourt and Vearncombe, 1992). The Thabazimbi-Murchison Lineament (TML, Figs. 2, 6 and 7), a deformation belt with a long-lived tectonic history, is one such feature roughly

25 km wide that stretches for approximately 500 km across the Kaapvaal craton (Good and de Wit, 1997). The TML appears to be an important controlling structure for the SKS shear-wave splitting results and, to a lesser degree, for the MT results.

3. Seismic anisotropy (shear-wave splitting)

The following is intended as a brief description of shear-wave splitting; for more complete reviews of the methodology see Silver (1996) and Savage (1999). A seismic shear wave that passes through a seismically anisotropic medium is split into different polarisation directions that have differing propagation velocities. The so-called SKS shear-wave splitting studies utilise near-vertical wave paths of seismic energy from teleseismic events that pass through the core, and they provide us with a means of indirectly measuring the deformation in the crust and mantle. The method has been used in many studies worldwide, particularly since the early 1990s (see review by Savage, 1999). In shear-wave splitting studies the measured splitting parameters are the fast polarisation direction (ϕ_S) indicating the orientation of deformation, and the delay time (δt) between the perpendicularly polarised fast and slow arrivals, indicating the magnitude of deformation in the horizontal plane (Silver, 1996). This method provides good lateral resolution, but has no intrinsic vertical resolution—the anisotropy could reside anywhere on the path from the core-mantle boundary to the surface.

Seismic anisotropy in the upper mantle is predominantly interpreted to arise from the preferred orientation of anisotropic crystals as result of mantle deformation caused by past and present geological processes (Silver, 1996). Olivine, being the most abundant phase in the upper mantle, is an anisotropic crystal whose orientation is strain dependent, known as lattice preferred orientation (LPO), and is expected therefore to reflect these deformational processes. Vinnik et al. (1992) correlate absolute plate velocity directions with the fast direction of seismic anisotropy in the upper mantle, and suggest that the dominant cause of the observed SKS anisotropy is due to recent and present-day flow in the mantle, though this hypothesis does not always appear to be consistent with observations (e.g., Silver et al., 2001). The diametrically opposed counter-hypothesis is that of Silver and Chan (1988, 1991), who suggest that SKS anisotropy is dominantly a response to fossil, or frozen-in, crystal alignment created at the time of primary lithospheric formation. There are further complexities to these arguments that have been explored in more recent work (e.g., Jung and Karato, 2001; Holtzman et al., 2003) and suggest that the alignment depends significantly on the region being studied. Jung and Karato (2001) show that the addition of large amounts of water to olivine (e.g. in subduction zones) can change the relation between flow geometry and seismic anisotropy. Additionally, Holtzman et al. (2003) demonstrate that the presence of melt weakens the alignment of the olivine fast axis (also know as the *a* axis, or [1 0 0] axis), and where the melt segregates to form networks of shear zones it may even cause the alignment to be at 90° to the shear direction. Neither of these mechanisms, however, is expected to be operative in Archean or Proterozoic-aged lithosphere.

Silver et al. (2001) inferred single-layer seismic anisotropy from shear-wave splitting at 79 sites in southern Africa of the SASE deployment. They divided the results from the analyses into three categories: well-constrained stations that showed resolvable splitting, stations that did not exhibit detectable splitting, and stations that were poorly constrained (Fig. 2). Overall, where splitting was observed, delay-times are small (typically 0.6 s) compared to world averages (1–2 s). Silver et al. (2001, 2004) showed that the absolute plate motion (APM) of southern Africa does not explain the polarisation directions (ϕ) that are derived, contrary to the Vinnik et al. (1992) hypothesis, but rather that the orientation direction of the anisotropy (fast polarisation direction) is more closely aligned with the strike of known Archean-aged deformational structures of the Kaapvaal craton. The depth of the anisotropic region was concluded to be confined to the lithospheric mantle, with (a) the lack of correlation of the anisotropy directions with APM models resulting in the asthenosphere being excluded as a causative region and with (b) conversions at the crust-mantle boundary being exploited to exclude crustal effects. There appears to be strong differences in both the splitting parameters between early and late Archean regions of the craton, as well as between on and off craton regions. These results provide support for the hypothesis that mantle deformation is preserved from events as far back as the age of the Earth's earliest continental cratonic fragments.

4. Electrical anisotropy

Gaining an understanding of the geoelectric dimensionality and directionality in a dataset is the first step in the analysis of MT data, and enhances our understanding of the electrical anisotropy, in the broadest sense of the term including micro and macro anisotropy as well as lateral heterogeneity, of the survey region. In a similar manner to the SKS approach, electrical anisotropy is represented by the direction of maximum conductivity (ϕ_E), which is either parallel or perpendicular to the regional strike direction (see below for discussion). The processed MT responses are in the form of a frequency-dependent 2×2 complex impedance tensor, the elements of which can be transformed into magnitudes, scaled as apparent resistivities, and phases. In most situations, the most important tensor elements are the off-diagonal ones which relate the horizontal magnetic field components to their perpendicular electric field components. For a one-dimensional (1-D) Earth, the diagonal terms are zero and the off-diagonal terms are equal to each other (except for a sign difference). For a two-dimensional (2-D) Earth, in strike coordinates the diagonal terms are zero and the off-diagonal terms are different from each other. When the impedance tensor cannot be validly described by either of these, then the Earth is three-dimensional (3-D), or is 1-D or 2-D but with galvanic distortion effects (see below). In addition to a magnitude relationship, akin to apparent resistivity in DC methods, we derive the phase of an impedance tensor element, which is the phase lead of the electric field over the magnetic field. In 2-D when in strike coordinates, where the phase difference ($\delta\theta$) between the two off-diagonal elements of the impedance tensor is small it implies there is little lateral heterogeneity in the subsurface, i.e., almost 1-D, compared with a larger phase difference, which is indicative of 2-D or 3-D regional structures.

In MT soundings local, small-scale conductivity heterogeneities cause distortions of primarily the electric field, and deform the response produced by the underlying, regional geoelectric structures. In the ideal, distortion-free 2-D case the diagonal elements of the impedance tensor would be zero when rotated to the appropriate strike direction; though with experimental data, this is rarely, if ever, the case. The distortions can be practically (though not entirely separately) viewed as inductive and galvanic effects. The inductive effect is a result of the time-varying magnetic field that induces currents, which, if flowing in closed loops, will in turn result in a secondary magnetic field that adds to the primary magnetic field (Jones, 1988; Jiracek, 1990). Where there are local conductivity heterogeneities in the subsurface, flux through the boundaries of these heterogeneities by the regional current results in the build-up of charge at these boundaries (Price, 1973, see also Jones, 1983a) as a consequence of Ohm's Law. These charges create a secondary electric field that distorts the regional current flow in that area. Where the distorting inhomogeneity is small relative to the scale size of the experiment, this effect is known as galvanic distortion. Such distortion may also be caused by topography near the measurement location (Jiracek, 1990). Galvanic distortion effects persist to the longest periods, whereas the effect of near-surface inductive distortions decreases in proportion to the regional inductive response with increasing period (Jones and Groom, 1993; Chave and Smith, 1994; Chave and Jones, 1997; Smith, 1997; Agarwal and Weaver, 2000). At sufficiently long periods, where "sufficient" is defined by the inductive scale length of the distorting structures, except for unusual cases of intense distortion to the regional current density, the horizontal magnetic field components are largely unaffected (Groom and Bailey, 1989; Chave and Jones, 1997; Caldwell et al., 2004), and the distortion effect is almost entirely limited to the electric field.

There are a number of methods that are used for galvanic distortion analysis of MT data; accordingly there are also a number of reviews on the subject of how to address the problem (e.g., Jiracek, 1990; Groom and Bahr, 1992; Groom et al., 1993; McNeice and Jones, 2001). Two of the more commonly used methods are Bahr (1988), and Groom and Bailey (1989), both of which are 2-D extensions of the 1-D approach of Larsen (1977). Richards et al. (1982) were the first to propose this approach for handling galvanic distortions of the electric field from 2-D regional structures. Unfortunately, their paper is rather inaccessible, with the result that those authors have not received the recognition due for their insight.

Both the Bahr and Groom–Bailey (GB) methods recover parameters from the magnetotelluric impedance tensor, and assume that the regional conductivity structure that we are attempting to resolve is either 1-D or 2-D, but not 3-D. Utada and Munekane (2000) and Garcia and Jones (2001) considered 3-D galvanic distortion of EM fields from 3-D regional structures, and proposed methods for its examination, but application of these approaches is not yet routine. The parameters that are obtained from the GB approach (the so-called twist, shear, and anisotropy tensors) are a consequence of a matrix factorisation of the distortion tensor and partially describe the effects of distortion. The GB approach has the distinct advantage over Bahr's parameterisation, and that of Smith (1995, 1997) and earlier factorisations (Eggers, 1982; Spitz, 1985; LaTorraca et al., 1986), in that the parameterisation is in terms of determinable and indeterminable parts, rather than a complex (and, for some factorisations, unknown) mix of the two. In our analysis we use the extended GB approach of McNeice and Jones (2001), where a minimum is sought in order to find the appropriate regional geoelectric strike direction and telluric distortion parameters for a range of frequencies at each site.

Phase tensor analysis is another, more recently developed, method of determining the dimensionality of the subsurface conductivity distribution (Caldwell et al., 2004). The phase relationships that are contained in the impedance tensor are shown by Caldwell et al. (2004) to be a second-rank tensor. This second-rank phase tensor, contained within the impedance tensor, is non-symmetric in the 3-D case and has a third coordinate invariant, which is a distortion-free measure of asymmetry found in the regional magnetotelluric response. We have used this method in order to compare with the results obtained through the GB approach.

There are a number of suggested causes for electrical anisotropy that gives rise to the regionally observed effect; however, as yet there is little consensus on the causative phenomenon. Hydrogen diffusion has been proposed as a mechanism for reducing electrical resistivity of mantle materials (Karato, 1990; Hirth et al., 2000), and recent laboratory studies are showing that minor (a few hundred ppm) amounts of water are sufficient to raise the electrical conductivity of olivine by several orders of magnitude (Poe et al., 2005). Anisotropic hydrogen diffusivity in olivine crystals (the most abundant mineral in the upper mantle) has been suggested as an explanation for electrical anisotropy, with the [1 0 0] axis of the olivine crystal having the highest rate of diffusion, therefore being the more conductive (Schock et al., 1989; Mackwell and Kohlstedt, 1990); however, this effect is thought to account for only about a third of the average measured values at most (Simpson and Tommasi, 2005). This indicates that there must be other factors, larger in magnitude of effect compared with the olivine crystal scale, which contribute to the overall electrical conductivity that we are observing. One such possibility would be interconnectivity of a conductive mineral phase (e.g., graphite) along grain boundaries, and therefore along foliations and lineations, referred to as shape-preferred orientation (Mareschal et al., 1995; see Jones, 1992, for a more complete discussion in this regard). Saline fluid-filled cracks are another possibility that has been suggested and is one that would likely affect both seismic and electrical anisotropy; however, this would most likely be a mechanism valid only in the crust.

It must be noted that from MT data alone it is virtually impossible to discriminate between the response to a 2-D structure (heterogeneity), such as a fault in the lower crust, and the response due to 2-D anisotropy that is of a scale not resolvable by the technique. The difference between the two can however be observed in the response of the vertical magnetic field (Cull, 1985; Mareschal et al., 1995; Jones, 1999). More detailed discussions on the topic of heterogeneity versus anisotropy and some of the problems that anisotropy poses are described by Heise and Pous (2001) and in the recent review by Wannamaker (2005).

5. The symbiotic relationship

One of the most problematic areas for seismic SKS analysis is vertical resolution, caused by the use of seismic waves with near-vertical ray paths and long wavelengths for analysis. The advantage of using such ray paths is that, depending on the quantity and quality of the data that are collected, horizontal resolution within the lithosphere can be exceptionally good (<50 km, Savage, 1999). However, without additional information vertical resolution is extremely poor. Conversely, the magnetotelluric (MT) method has intrinsic vertical dependency due to the skin depth phenomenon, which assures penetration at any depth depending on the period and resistivity (ρ) of the subsurface. In theory, to penetrate deeper into the Earth, all one needs to do is to measure at sufficiently longer periods, although at great depths source field geometry needs to be taken into account (e.g., Jones and Spratt, 2002), and the exponential sensitivity of impedance skin depth results in a decrease in resolution with depth, thereby also causing a loss of vertical resolution with depth.

Although these two methods, SKS shear-wave splitting and MT, do not measure the same physical properties, in certain cases it may be the case that they are essentially measuring a different response of the same causative effect. As an example of this, Ji et al. (1995) noted a directional obliquity between MT and seismic anisotropy results, and suggested that the cause for this was the differing directions of lattice-preferred (LPO) and shape-preferred (SPO) orientations of mantle minerals. They used this obliquity result to suggest that a combination of both MT and SKS results could be employed to determine the sense of movement of transcurrent ductile shear zones in the upper mantle. They concluded that although the direct cause of the anisotropy was different for the two methods, they were a result of the same tectonic feature. Following up on this hypothesis, Eaton et al. (2004) conducted an experiment across a highly sheared region, the Great Slave Lake shear zone of northern Canada. They correlated MT anisotropy with seismic (SKS and SKKS) anisotropy to constrain the depth location of the seismic anisotropy using approximately collocated teleseismic and magnetotelluric observations. They noted that in their study region there was no systematic obliquity observed between the MT and seismic results, but suggested that this may be because of the intense deformation of the Great Slave Lake shear zone resulting in parallel axes for the C (shear band) and S (foliation fabric) strain ellipses.

Another recent MT/SKS comparison study by Padilha et al. (2006) has shown that in parts of the survey area (central south-eastern Brazil) where there is significant electrical anisotropy, a close correlation of shear-wave splitting results and MT strike results can be made, also without any systematic obliquity. They deduce from their study that lithospheric and sublithospheric deformation is vertically coherent with the surface tectonic trends in this region, which requires strong crust-mantle coupling across the Moho and is indicative of the lack of a lower crustal rheologically weak layer. From these studies it is clear that MT is indeed an exquisitely complementary method to seismic methods for mantle imaging (Jones, 1999); however, the use of both methods together for combined interpretations is still in its infancy, and certainly the implications of the correlations are immature.

There are a number of suggested causes for electrical and seismic anisotropy, some of which have been discussed earlier. The explanation most readily used for upper mantle seismic anisotropy is strain-induced LPO of olivine crystals (see reviews by Silver, 1996, and Savage, 1999, and references therein). In the lower crust, aligned saline fluid-filled cracks may account for anisotropy, and would affect both seismic and electrical results, but this does not readily explain observations of lithospheric mantle anisotropy. There does not appear to be a general consensus on the causes of electrical anisotropy, largely because there are insufficient observations, and those made to date are highly area dependent implying a combination of causes. For example, in a highly ordered upper mantle it is possible that anisotropic hydrogen diffusivity is a contributing factor, but this is unlikely to be either the dominant factor or the sole cause. Even when present it likely will result in an electrical anisotropy factor no greater than about 3–4. Thus, to aid us in the meaningful interpretation of seismic and MT observations of anisotropy we must rely heavily on geological knowledge, such as geochemical and petrological results.

6. MT data analysis

Data from the main SAMTEX Kaapvaal craton profile, from Southerland in the southwest of South Africa to Messina at the South Africa–Zimbabwe border (Fig. 1), have been analysed for anisotropy using the McNeice and Jones (2001) distortion decomposition code, and the results compared with applying phase tensor analysis (Caldwell et al., 2004). This survey line, the first to be undertaken in the SAMTEX program, is almost 1500 km in length and extends over important and diverse geological terranes, including the Kaapvaal craton (mainly the western section), the Limpopo belt, and the Namaqua-Natal mobile belt. As could be expected due to the length of the survey, data quality is variable, with the southwest of the line producing the highest quality responses, while sites near Kimberley were the lowest quality, being seriously affected by DC train noise.

Due to the large scale of the survey it is necessary to consider that penetration over the various regions will differ significantly; for example depth penetration at long periods on the Karoo Basin and on the Bushveld Complex is highly attenuated due to their high upper crustal conductivity compared with other regions. In order to gain a quantitative understanding of this issue, we estimated the frequency for penetration to given depths using Niblett–Bostick (Niblett and Sayn-Wittgenstein, 1960; Bostick, 1977; Jones, 1983b) depth estimates (Fig. 3) and inductive response functions, also known as C response functions (Schmucker, 1970; Jones, 1980). The real part of the C response function, related to MT impedance by a factor of $1/\omega\mu$, was shown to be the depth of maximum eddy current flow by Weidelt (1972), and is a measure of the depth of investigation. Three-dimensional structures that may influence the C responses are assumed to be sufficiently long at the depth of investigation such that they may be interpreted as being 2-D; additionally the decomposition analysis determines whether a 2-D assumption is valid. The penetration information in Fig. 3 was calculated using Niblett–Bostick estimates (which are almost identical to the C response function estimates) on distortion-removed data in order to minimise the influence of distortion on the calculations. Static shift effects are not corrected by distortion analysis and can influence depth estimates by the square root of their value (e.g., Jones, 1988), definitely not as severe as on apparent resistivity data. Notwithstanding the possible presence of static shift effects, there are clearly regional trends visible in the data. Note the significance of this figure (Fig. 3); electromagnetic waves penetrating to 35 km in the crust are at periods of 1000 s or greater at the southern (stations 1–30 on the Karoo Basin) and north-central (stations 46–56 on the conductive Bushveld Igneous Complex) sites, at periods of 2 s or less in the centre (stations 30–45 in the centre of the Kaapvaal craton) of the profile, and at periods of 30 s or less at the northern end of the profile (stations 57–75, NE Kaapvaal craton and Limpopo mobile belt). Clearly, a map of geoelectric strikes from these stations at one particular period would be meaningless, as depth penetration varies significantly along the profile. The effect is a direct consequence of the large variation of the

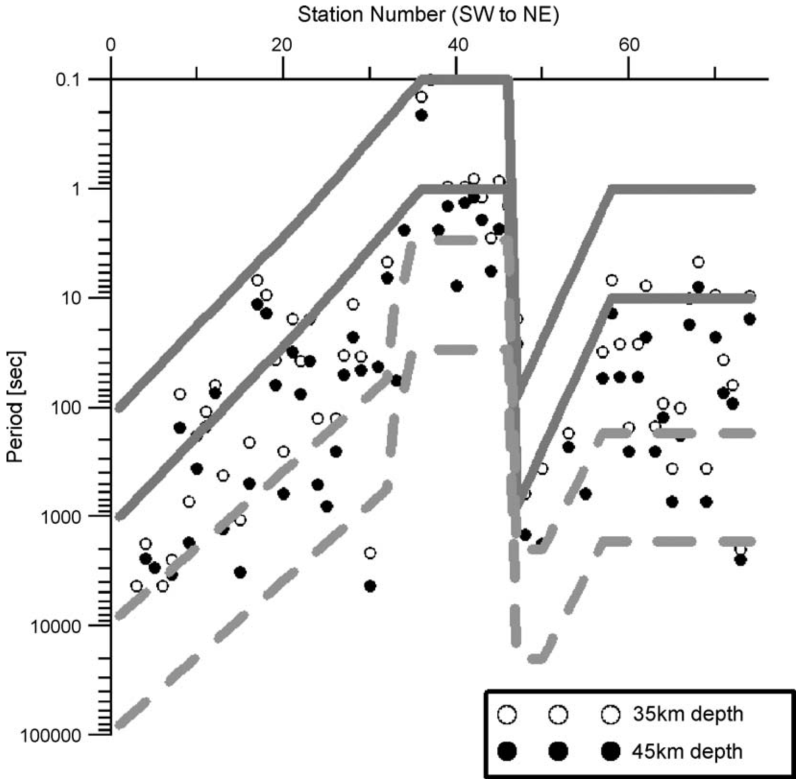

Fig. 3. The corresponding period (averaged between the two modes) for depths of 35 km and 45 km determined using Niblett–Bostick depth estimation on distortion-removed data. This gives an indication of the variation in penetration depth along the profile. Note the sudden drop in penetration around station 48 as we move onto the very conductive Bushveld Igneous Complex (BIC). The period decade between the two solid lines indicates the frequencies used to estimate the strike directions for crustal depths, while the period decade between the two dashed lines indicates the frequencies used to estimate the strike directions for upper mantle depths.

parameter that EM studies are sensing, namely electrical resistivity, which ranges over many orders of magnitude (see, e.g., Jones, 1992), and contrasts sharply with the small (less than 10%) variations in seismic parameters. From these results it is clear that either the line must be split into sections and analysed separately, or the data must be analysed for given depths, as opposed to given frequencies, in order to make interpretation of any resulting strike map meaningful. Jones (2006) raises this caution and shows examples from three other regions of the world where one must give consideration to penetration depth.

Crustal thickness, as defined by the seismic results (Nguuri et al., 2001; Stankiewicz et al., 2002; James et al., 2003), varies from ∼35–40 km below the craton, to ∼45–50 km below the Proterozoic regions where the Moho is also more complex. In order to gain strike directions representative of the crust and upper mantle, while avoiding complex structures at the crust-mantle boundary, we selected a one-decade wide period band for the crust (between the two solid lines on Fig. 3) and the upper mantle (between the two dashed lines on Fig. 3). One-decade wide bands were selected so as not to bias any one site with more or less data than another. These sites were then each analysed twice (separately for each frequency band) using the single site GB approach (Groom and Bailey, 1989) for a range of frequencies, as implemented by McNeice and Jones (2001), in order to determine two regional geoelectric strike estimates for each site, one representative of the crust and one representative of the upper mantle. Data were analysed with an assumed error floor of 2° for the phase and equivalent 7% for apparent resistivity. The average calculated RMS values from the unconstrained, one-decade wide GB decomposition for most sites were in the range between one and three for both the crustal and upper mantle analyses. The average twist values were mostly within the range ±30°, and the shear values were generally slightly higher falling within the range ±40°. Both the twist and shear values were slightly higher at the longer periods (upper mantle band), where the signal to noise ratios are worse. The average RMS, twist, and shear results for all the sites, are displayed in Fig. 4 (crustal results on the left and mantle results on the right), which shows that the

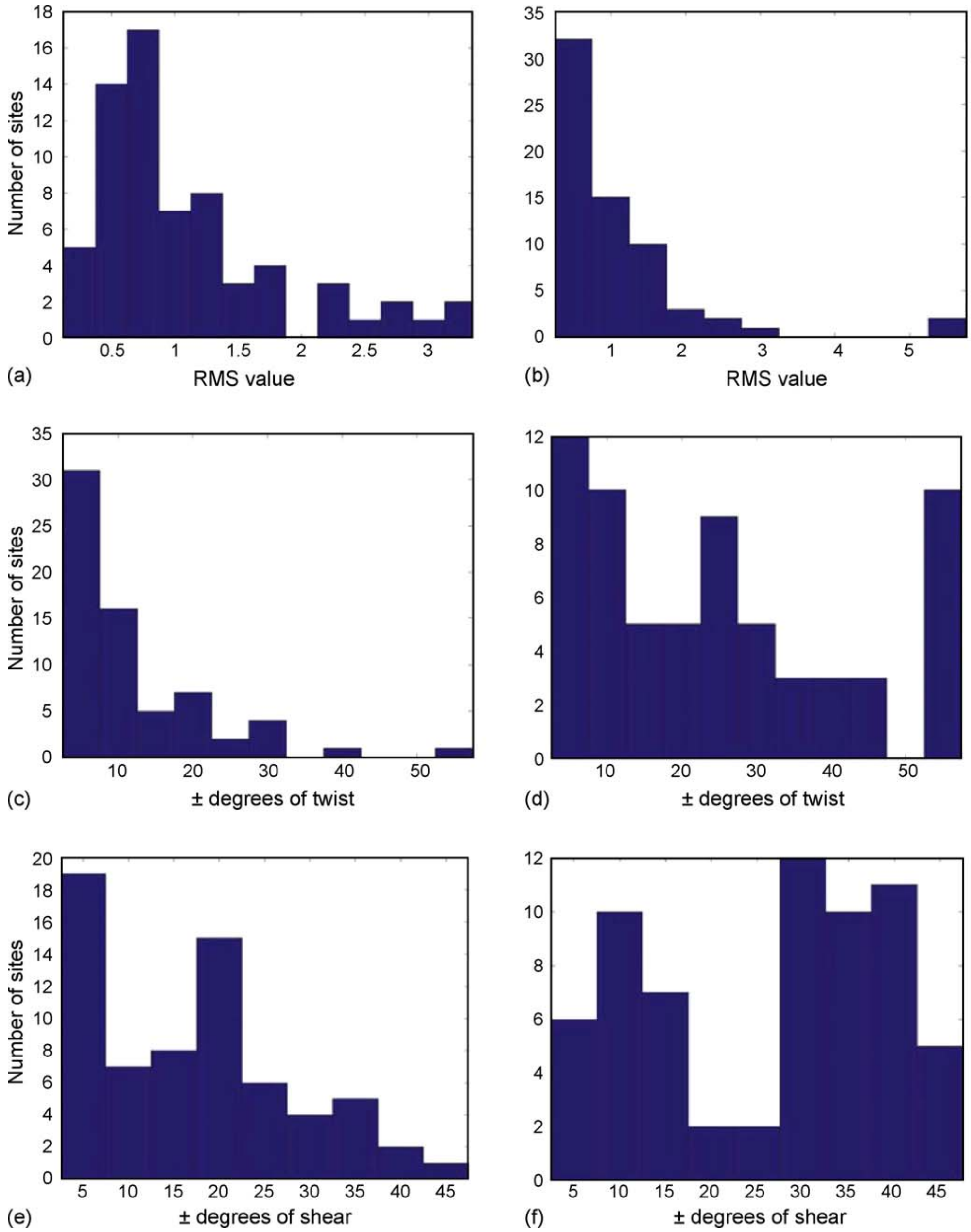

Fig. 4. Histograms displaying results from Groom–Bailey (GB) decomposition analyses. Displayed are: (a, b) the average RMS values, (c, d) the average (positive or negative) twist (in degrees), and (e, f) the average (positive or negative) shear (in degrees), for all the sites. Histograms for the crustal band are on the left (a, c, e), and for the upper mantle band on the right (b, d, f).

majority of the data have reasonably low distortion values compared to what can often be observed on shield regions e.g., Fennoscandian Shield (Lahti et al., 2005). For these data, the direction chosen to display as geoelectric "strike" was taken as the more conductive direction of the two. This direction was reasonably consistent with that found using the phase tensor approach (Caldwell et al., 2004), as is to be expected for high-quality, low noise, low distortion data. The GB approach proves itself superior in the presence of higher noise and/or higher distortion, e.g., Jones and Groom (1993), McNeice and Jones (2001).

However, the more conductive direction is not necessarily the strike direction of 2-D structures. Consider the TE and TM apparent resistivity curves for a simple two quarter-space fault model (e.g., d'Erceville and Kunetz,

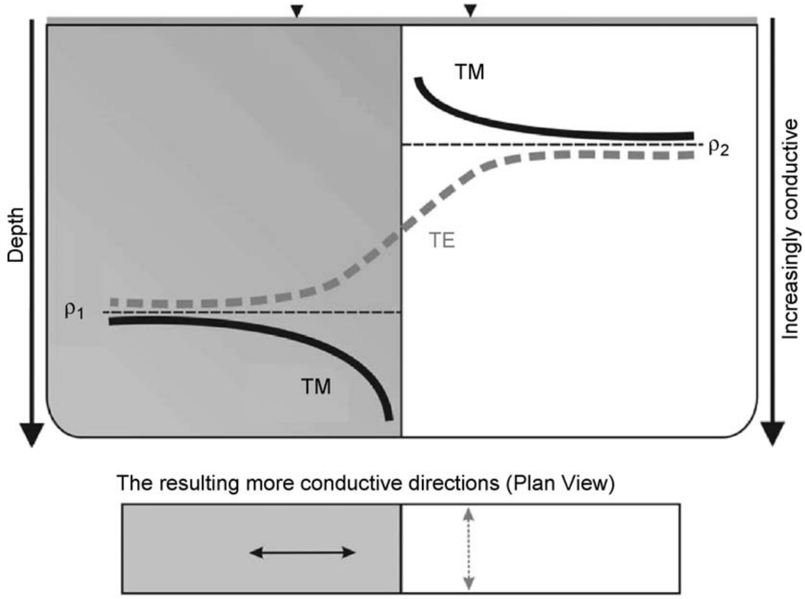

Fig. 5. Schematic diagram portraying the MT response at one frequency to the two quarter-space fault model with the more conductive side shaded grey. The variations of the TE and TM modes across the fault for a given frequency are shown. On the more conductive side of the fault, the TM mode apparent resistivity is the more conductive, whereas on the resistive side of the fault the TE mode apparent resistivity is the more conductive. This results in the more conductive directions being parallel to the geological strike on one side of the fault (the resistive side), and perpendicular on the other (the conductive side).

1962; Weaver, 1963; Price, 1973), schematically drawn in Fig. 5. On the resistive side of the fault the TE mode apparent resistivity is the more conductive (lower resistivity), so its direction is taken, which is correctly the strike direction of the fault as the TE electric field is parallel to strike. Conversely, on the conductive side of the fault (shaded side in Fig. 5), the TM mode apparent resistivity is the more conductive, so its direction is taken, which is perpendicular to strike. Herein we are concerned only with the more conductive direction and its correlation with the faster shear velocity direction. It is important to appreciate that we are not using these conducting directions to define geological strike for a 2-D interpretation.

The geoelectric strike directions for the crust (<35 km) and upper lithospheric mantle (>45 km) are shown as red lines in Figs. 6 and 7, respectively, together with the terrane subdivision of southern Africa from potential field data. The lines are scaled by the maximum phase difference in the frequency band analysed, as a proxy for the amplitude of anisotropy. Some sites were omitted from the plot if either there were no data at sufficiently long periods, or if the data at the periods analysed were very poor (high noise content or large error bars). The geoelectric upper mantle strike results (Fig. 7) fall within the probable causative region of the seismic anisotropy, which was confined through inferences of the seismic results. On Fig. 7 are also plotted the seismic anisotropy results of Silver et al. (2001) for comparison.

7. Discussion

Bearing in mind the physics of the model described in Fig. 5, the crustal MT results (Fig. 6) display some interesting and satisfying, though obviously complex, features. The more conductive directions at the southwestern craton boundary are parallel to the boundary on the Namaqua-Natal mobile belt (NN), but upon moving onto the craton the directions change abruptly to be nearly perpendicular to the NN. This behaviour is consistent with Fig. 5, implying that the Kaapvaal craton crust is more conducting than the Namaqua-Natal crust, and is what we would expect if large-scale 2-D geologic features were responsible for the electrical structure. Similar orthogonal relationship patterns can be observed at the Colesburg Magnetic Lineament (CML, blue line on Fig. 6), the Thabazimbi-Murchison Lineament (TML, purple line on Fig. 6), as well as at the Kaapvaal craton–Limpopo belt boundary. The results to the immediate SW of the TML are complex, and are probably a result of the influence of the conductive Bushveld Igneous Complex (BIC). At first glance, the result from the site on the end of the profile in the SW

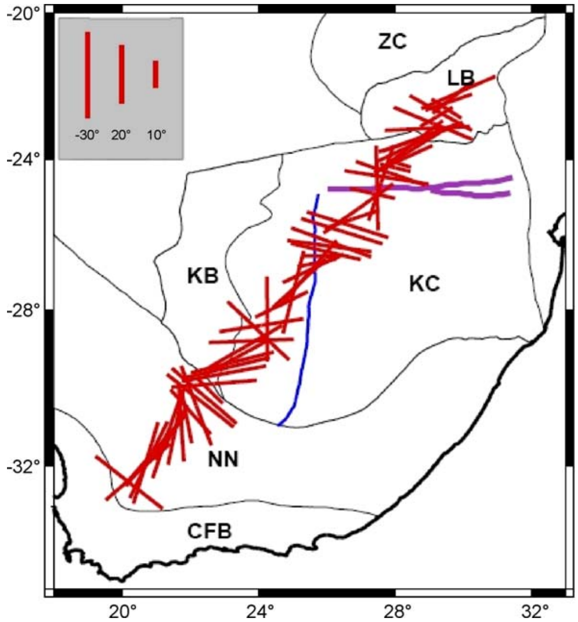

Fig. 6. Electrically more conductive directions (in red), scaled by maximum phase difference, for the crust. ZC: Zimbabwe craton. KC: Kaapvaal craton. LB: Limpopo belt. NN: Namaqua-Natal mobile belt. CFB: Cape Fold belt. KB: Kheis and Proterozoic fold and thrust belt. Purple lines: the E–W trending Thabazimbi-Murchison Lineament (TML), as plotted by Silver et al. (2001). Blue line: the N–S trending Colesburg Magnetic Lineament (CML). (For interpretation of the references to colour in this figure legend, the reader is referred to the web version of the article.)

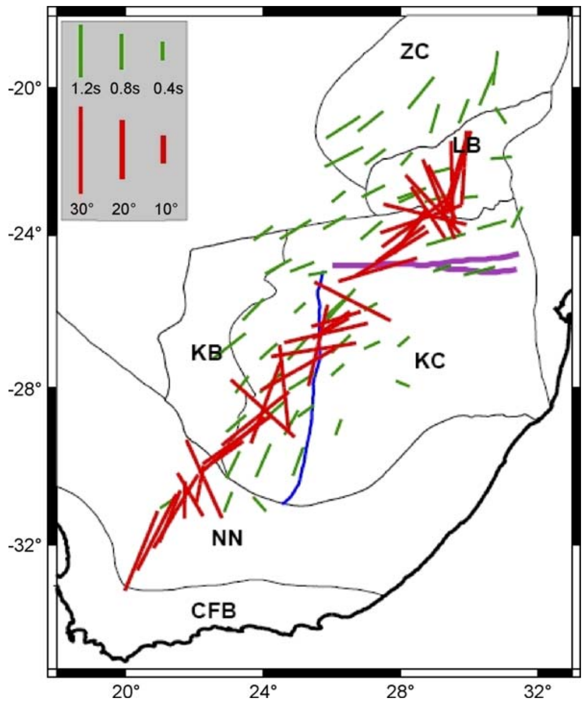

Fig. 7. Electrical more conductive directions (in red), scaled by maximum phase difference, for the lithospheric upper mantle, and the shear-wave splitting results (both high and low quality results plotted in green, but sites with no detectable splitting omitted). ZC: Zimbabwe craton. KC: Kaapvaal craton. LB: Limpopo belt. NN: Namaqua-Natal mobile belt. CFB: Cape Fold belt. KB: Kheis and Proterozoic fold and thrust belt. Blue line: the N–S trending Colesburg Magnetic Lineament (CML). Purple lines: the E–W trending Thabazimbi-Murchison Lineament (TML), as plotted by Silver et al. (2001). (For interpretation of the references to colour in this figure legend, the reader is referred to the web version of the article.)

seems anomalous; however, it may be that this site is being affected by a response from the Cape Fold belt (CFB), although no data were collected further towards and onto the CFB to confirm this.

The upper mantle MT results (Fig. 7, red lines) do not correlate well with those from shear-wave splitting (Fig. 7, green lines). The close azimuthal correlations between geoelectric strike and seismic fast-axis directions noted by other authors (e.g. Eaton et al., 2004; Padilha et al., 2006) are not observed in our data, nor do we see a constant obliquity between the two results, as observed by Ji et al. (1995). A few sites, particularly those around the TML and to the SW of the profile, do show distinctly similar directions to the seismic results; however, overall the results are far too inconsistent to draw any reliable conclusions about their correlation. The same effect of Fig. 5, although not as clear as in the crustal results, can be observed at the craton boundaries, indicating that these features are distinct at upper mantle depths and that there is probably strong coupling between the crust and upper mantle. Results near the TML do not show the same effect, suggesting that this feature is confined to the crust. A similar argument could be applied for the CML, although the results in this region are confusing and seem to lack any discernible order. Unfortunately the site furthest to the SW that seemed to respond to the CFB in the crustal analysis did not have data at sufficiently long periods to probe upper mantle depths and consequently we can make no further judgement on this. A noteworthy feature is the N–S geoelectric directions for the northeast-most stations. There is no correlation between these sites and the surface geological trends of the Limpopo belt, nor the surrounding seismic fast-axis directions. However, to the north the seismic fast-axis directions do follow the same N–S trend. This effect was attributed by Silver et al. (2001) to the Great Dyke of Zimbabwe, which has a general N–S trend across the country. Is it possible the electrical response to this massive feature is sensed at further distances than the seismic response? An answer to this question can only come through future MT measurements in Zimbabwe.

Our crustal geoelectric strike results are clearly a result of large-scale geological structures. The upper mantle MT anisotropy direction results show little correlation with the seismic SKS anisotropy results. We observe rather large phase differences, of the order of 20° or more, that are difficult to achieve with the low order of anisotropy expected from hydrogen diffusion in aligned olivine grains. Were these large phase differences caused by the response to an interconnecting conductive mineral phase along lineation or foliation planes, we would expect the results to correlate better with the seismic results, if not exactly, then with a constant obliquity such as observed by Ji et al. (1995). Following this reasoning, there are a few possible explanations for the upper mantle MT results we observe: either the effect of the large-scale 2-D geological structure is "hiding" the lesser magnitude effect due to preferentially aligned crystals or an interconnecting mineral phase; perhaps there is no corresponding electrical response to the cause of the seismic shear-wave splitting results; or the causative layer of the seismic response could reside deeper in the lithosphere, beyond the depths that we are sensing.

Our MT profile is located mainly across the younger western section of the Kaapvaal craton, and thus at this stage we are unable to draw any conclusions as to whether we see similar variations in on-craton geological regions to those observed by the shear-wave splitting results. The phase differences do not appear to show any correlation between the different geological regions, though trends are expected to appear when the newer SAMTEX data, continuing into other regions of the craton and into more of the surrounding geological provinces, have been analysed. Analyses of data from the surrounding areas are bound to yield some interesting outcomes that will be integrated with the Kaapvaal Craton Project.

8. Conclusions

Our crustal electrical anisotropy results are quite instructive, and rather satisfying. They appear to be strongly related to large-scale geological structures both at craton and surrounding terrane boundaries as well as within the craton itself. Some of these features such as the TML are confined to the crust, while others such as the craton boundaries are distinct at upper mantle depths.

The electrical results for the upper lithospheric mantle do not appear to correlate well with the shear-wave splitting results for the same region. Thus, if aligned olivine is the cause of the observed seismic anisotropy, it is not the cause of the observed electrical anisotropy. We conclude that the cause of the electrical response at these depths is dominantly as a result of large-scale geological structures, although there may be contributions smaller in magnitude from preferential crystal alignment or interconnecting mineral phases.

Acknowledgements

We would like to thank the whole SAMTEX Team, comprising many enthusiastic organisations and individuals, without whose colossal and unrelenting efforts this project would never have been possible. Especially we wish to thank the project financial sponsors, namely the National Science Foundation's Continental Dynamics program, the Council for Geoscience, Science Foundation Ireland, De Beers Group Services and Rio Tinto Mineral Exploration. Further details on the SAMTEX project and its participants can be found at http://www.dias.ie/~mh/SAMTEX.html.

We would like to thank Professors Andreas Junge, David W.S. Eaton, and an anonymous reviewer for their reviews and comment on the submitted paper. We would also like to thank S.J. Webb and K. Garcia for helpful reviews on the early version of the paper, and M. Moorkamp and C.K. Rao for their useful discussions during the preparation of this manuscript. All maps were produced using the program GMT (Wessel and Smith, 1991; Wessel and Smith, 1995), with some of the geological digitising obtained from S.J. Webb.

References

Agarwal, A.K., Weaver, J.T., 2000. Magnetic distortion of the magnetotelluric tensor: a numerical study. Earth Planets Space 52, 347–353.

Bahr, K., 1988. Interpretation of the magnetotelluric impedance tensor: regional induction and local telluric distortion. J. Geophys. 62, 119–127.

Bostick, F.X., 1977. A simple almost exact method of MT analysis. Workshop on Electrical Methods in Geothermal Exploration, U.S. Geol. Surv., Contract No. 14080001-8-359.

Caldwell, T.G., Bibby, H.M., Brown, C., 2004. The magnetotelluric phase tensor. Geophys. J. Int. 158, 457–469.

Carlson, R.W., Boyd, F.R., Shirey, S.B., Janney, P.E., Grove, T.L., Bowring, S.A., Schmitz, M.D., Dann, J.C., Bell, D.R., Gurney, J.J., Richardson, S.H., Tredoux, M., Menzies, A.H., Pearson, D.G., Hart, R.J., Wilson, A.H., Moser, D., 2000. Continental growth, preservation, and modification in southern Africa. GSA Today 10, 1–7.

Carlson, R.W., Grove, T.L., de Wit, M.J., Gurney, J.J., 1996. Program to study the crust and mantle of the Archean craton in southern Africa. EOS, Trans. Am. Geophys. Union 77, 273–277.

Chave, A.D., Jones, A.G., 1997. Electric and magnetic field distortion decomposition of BC87 data. J. Geomagn. Geoelectr. 49, 767–789.

Chave, A.D., Smith, J.T., 1994. On electric and magnetic galvanic distortion tensor decompositions. J. Geophys. Res. 99, 4669–4682.

Corner, B., Durrheim, R.J., Nicolaysen, L.O., 1990. Relationships between Vredefort structure and the Witwatersrand basin within tectonic framework of Kaapvaal craton as interpreted from regional gravity and aeromagnetic data. Tectonophysics 171, 49–61.

Cull, J.P., 1985. Magnetotelluric soundings over a Precambrian contact in Australia. Geophys. J. R. Astron. Soc. 80, 661–675.

Davis, W.J., Jones, A.G., Bleeker, W., Grütter, H., 2003. Lithospheric development in the Slave Craton: a linked crustal and mantle perspective. Lithos 71, 575–589.

d'Erceville, E.J., Kunetz, G., 1962. The effect of a fault on the earth's natural electromagnetic field. Geophysics 27, 651–665 (Reprinted in Vozoff, 1986, 221–235).

de Wit, M.J., Roering, C., Hart, R.J., Armstrong, R.A., de Ronde, C.E.J., Green, R.W.E., Tredoux, M., Peberdy, E., Hart, R.A., 1992. Formation of an Archaean continent. Nature 357, 553–562.

Eaton, D.W., Jones, A.G., Ferguson, I.J., 2004. Lithospheric anisotropy structure inferred from collocated teleseismic and magnetotelluric observations: Great Slave Lake shear zone, northern Canada. Geophys. Res. Lett. 31, L19614, doi:10.1029/2004GL020939.

Eggers, D.E., 1982. An eigenstate formulation of the magnetotelluric impedance tensor. Geophysics 47, 1204–1214.

Garcia, X., Jones, A.G., 2001. Decomposition of three-dimensional magnetotelluric data. In: Zhdanov, M.S., Wannamaker, P.E. (Eds.), Three-Dimensional Electromagnetics, vol. 35. Elsevier, Methods in Geochemistry and Geophysics, ISBN 0-444-50429-X, pp. 235–250.

Good, N., de Wit, M.J., 1997. The Thabazimbi-Murchison Lineament of the Kaapvaal Craton, South Africa: 2700 Ma of episodic deformation. J. Geol. Soc. Lond. 154, 93–97.

Groom, R.W., Bailey, R.C., 1989. Decomposition of magnetotelluric impedance tensors in the presence of local three-dimensional galvanic distortion. J. Geophys. Res. 94, 1913–1925.

Groom, R.W., Bahr, K., 1992. Corrections for near surface effects: decomposition of the magnetotelluric impedance tensor and scaling corrections for regional resistivities: a tutorial. Surv. Geophys. 13, 341–380.

Groom, R.W., Kurtz, R.D., Jones, A.G., Boerner, D.E., 1993. A quantitative methodology for determining the dimensionality of conductive structure from magnetotelluric data. Geophys. J. Int. 115, 1095–1118.

Heise, W., Pous, J., 2001. Effects of anisotropy on the two-dimensional inversion procedure. Geophys. J. Int. 147, 610–621.

Hirth, G., Evans, R.L., Chave, A.D., 2000. Comparison of continental and oceanic mantle electrical conductivity: is the Archean lithosphere dry? Geochem. Geophys. Geosyst. 1, 2000GC000048.

Holtzman, B.K., Kohlstedt, D.L., Zimmerman, M.E., Heidelbach, F., Hiraga, T., Hustoft, J., 2003. Melt segregation and strain partitioning: implications for seismic anisotropy and mantle flow. Science 301, 1227–1230.

James, D.E., Fouch, M.J., 2002. Formation and evolution of Archean cratons: insights from southern Africa. In: Fowler, C.M.R., Ebinger, C.J., Hawkesworth, C.J. (Eds.), The Early Earth: Physical, Chemical and Biological Development, vol. 199. Geological Society, London, Special Publications, pp. 1–26.

James, D.E., Fouch, M.J., VanDecar, J.C., van der Lee, S., the Kaapvaal Seismic Group, 2001. Tectospheric structure beneath southern Africa. Geophys. Res. Lett. 28, 2485–2488.

James, D.E., Niu, F., Rokosky, J., 2003. Crustal structure of the Kaapvaal craton and its significance for early crustal evolution. Lithos 71, 413–429.

Ji, S., Rondenay, S., Mareschal, M., Senechal, G., 1995. Obliquity between seismic and electrical anisotropies as a potential indicator of movement sense for ductile shear zones in the upper mantle. Geology 24, 1033–1036.

Jiracek, G.R., 1990. Near-surface and topographic distortions in electromagnetic induction. Surv. Geophys. 11, 163–203.

Jones, A.G., 1980. Geomagnetic induction studies in Scandinavia. J. Geophys. 48, 181–194.

Jones, A.G., 1983a. The problem of "current channelling": a critical review. Geophys. Surv. 6, 79–122.

Jones, A.G., 1983b. On the equivalence of the "Niblett" and "Bostick" transformations in the magnetotelluric method. J. Geophys. 53, 72–73.

Jones, A.G., 1988. Static shift of magnetotelluric data and its removal in a sedimentary basin environment. Geophysics 53, 967–978.

Jones, A.G., 1992. Electrical conductivity of the continental lower crust. In: Fountain, D.M., Arculus, R.J., Kay, R.W. (Eds.), Continental Lower Crust. Elsevier, pp. 81–143 (Chapter 3).

Jones, A.G., 1999. Imaging the continental upper mantle using electromagnetic methods. Lithos 48, 57–80.

Jones, A.G., 2006. Electromagnetic interrogation of the anisotropic Earth: Looking into the Earth with polarized spectacles. Phys. Earth Planet. Inter. 158, 281–291.

Jones, A.G., Groom, R.G., 1993. Strike angle determination from the magnetotelluric impedance tensor in the presence of noise and local distortion: rotate at your peril! Geophys. J. Int. 113, 524–534.

Jones, A.G., Spratt, J., 2002. A simple method for deriving the uniform field MT responses in auroral zones. Earth Planets Space 54, 443–450.

Jordan, T.H., 1975. The continental tectosphere. Rev. Geophys. 13, 1–12.

Jung, H., Karato, S., 2001. Water-induced fabric transitions in olivine. Science 293, 1460–1463.

Karato, S., 1990. The role of hydrogen in the electrical conductivity of the upper mantle. Nature 347, 272–273.

Lahti, I., Korja, T., Kaikkonen, P., Vaittinen, K., the BEAR Working Group, 2005. Decomposition analysis of the BEAR magnetotelluric data: implications for the upper mantle conductivity in the Fennoscandian Shield. Geophys. J. Int. 163, 900–914.

Larsen, J.C., 1977. Removal of local surface conductivity effects from low frequency mantle response curves. Acta Geodaet. Geophys. et Montanist. Acad. Sci. Hung. 12, 183–186.

LaTorraca, G.A., Madden, T.R., Korringa, J., 1986. An analysis of the magnetotelluric impedance for three-dimensional conductivity structures. Geophysics 51, 1819–1829.

Mackwell, S.J., Kohlstedt, D.L., 1990. Diffusion of hydrogen in olivine: implications for water in the mantle. J. Geophys. Res. 95, 5079–5088.

McCourt, S., Vearncombe, J.R., 1992. Shear zones of the Limpopo belt and adjacent granitoid-greenstone terrains: implications for late Archean collision tectonics in southern Africa. Precambrian Res. 55, 553–570.

McNeice, G.W., Jones, A.G., 2001. Multisite, multifrequency tensor decomposition of magnetotelluric data. Geophysics 66, 158–173.

Mareschal, M., Kellett, R.L., Kurtz, R.D., Ludden, J.N., Bailey, R.C., 1995. Archean cratonic roots, mantle shear zones and deep electrical anisotropy. Nature 373, 134–137.

Niblett, E.R., Sayn-Wittgenstein, C., 1960. Variation of electrical conductivity with depth by the magneto-telluric method. Geophysics 5, 998–1008.

Nguuri, T.K., Gore, J., James, D.E., Webb, S.J., Wright, C., Zengeni, T.G., Gwavava, O., Snoke, J.A., Kaapvaal Seismic Group, 2001. Crustal structure beneath southern Africa and its implications for the formation and evolution of the Kaapvaal and Zimbabwe cratons. Geophys. Res. Lett. 28, 2501–2504.

Padilha, A.L., Vitorello, Í., Pádua, M.B., Bologna, M.S., 2006. Deep anisotropy beneath central-southeastern Brazil constrained by long period magnetotelluric data. Phys. Earth Planet. Int. 158, 190–209.

Poe, B., Romano, C., Nestola, F., Rubie, D., 2005. Electrical conductivity of hydrous single crystal San Carlos olivine. Fall AGU, Abstract #MR41A-0895.

Price, A.T., 1973. The theory of geomagnetic induction. Phys. Earth Planet. Int. 7, 227–233.

Richards, M.L., Schmucker, U., Steveling, E., 1982. Entzerrung der Impedanzkurven von magnetotellurischen Messungen in der Schwäbischen Alb. In: Protokol über das 9 Kolloquium Elektromagnetische Tiefenforschung (Abstracts from 9th Electromagnetic Deep Sounding Symposium), Neustadt, Weinstraße, 22–26 March, pp. 27–40.

Savage, M.K., 1999. Seismic anisotropy and mantle deformation: what have we learned from shear wave splitting? Rev. Geophys. 37, 65–106.

Schmucker, U., 1970. Anomalies of Geomagnetic Variations in the South-western United States. Bull. Scripps Inst. Oceanogr., Univ. Calif. Press, p. 13.

Schock, R.N., Duba, A.G., Shankand, T.J., 1989. Electrical conduction in olivine. J. Geophys. Res. 94, 5829–5839.

Silver, P.G., 1996. Seismic anisotropy beneath the continents: probing the depths of geology. Ann. Rev. Earth. Planet. Sci. 24, 385–432.

Silver, P.G., Chan, W.W., 1988. Implications for continental structure and evolution from seismic anisotropy. Nature 335, 34–39.

Silver, P.G., Chan, W.W., 1991. Shear wave splitting and subcontinental mantle deformation. J. Geophys. Res. 96, 16,429–16,454.

Silver, P.G., Fouch, M.J., Gao, S.S., Schmitz, M., the Kaapvaal Seismic Group, 2004. Seismic Anisotropy, mantle fabric, and the magmatic evolution of Precambrian southern Africa. S. Afr. J. Geol. 107, 45–58.

Silver, P.G., Gao, S.S., Liu, K.H., the Kaapvaal Seismic Group, 2001. Mantle deformation beneath southern Africa. Geophys. Res. Lett. 28, 2493–2496.

Simpson, F., Tommasi, A., 2005. Hydrogen diffusivity and electrical anisotropy of a peridotite mantle. Geophys. J. Int. 160, 1092–1102.

Smith, J.T., 1995. Understanding telluric distortion matrices. Geophys. J. Int. 122, 219–226.

Smith, J.T., 1997. Estimating galvanic-distortion magnetic fields in magnetotellurics. Geophys. J. Int. 130, 65–72.

Spitz, S., 1985. The magnetotelluric impedance tensor properties with respect to rotations. Geophysics 50, 1610–1617.

Stankiewicz, J., Chevrot, S., van der Hilst, R.D., de Wit, M.J., 2002. Crustal thickness, discontinuity depth, and upper mantle structure beneath southern Africa: constraints from body wave conversions. Phys. Earth Planet. Int. 130, 235–251.

Utada, H., Munekane, H., 2000. On galvanic distortion of regional three-dimensional magnetotelluric impedances. Geophys. J. Int. 140, 385–398.

Vinnik, L.P., Makeyeva, L.I., Milev, A., Usenko, A.Y., 1992. Global patterns of azimuthal anisotropy and deformations in the continental mantle. Geophys. J. Int. 111, 433–447.

Vozoff, K. (Ed.), 1986. Magnetotelluric Methods. Soc. Expl. Geophys. Reprint Ser. No. 5, Tulsa, OK, ISBN 0-931830-36-2.

Wannamaker, P.E., 2005. Anisotropy versus heterogeneity in continental solid earth electromagnetic studies: fundamental response characteristics and implications for physicochemical state. Surv. Geophys. 26, 733–765.

Weaver, J.T., 1963. The electromagnetic field with a discontinuous conductor with reference to geomagnetic micropulsations near a coastline. Can. J. Phys. 41, 484–495.

Weidelt, P., 1972. The inverse problem of geomagnetic induction. Z. Geophys. 38, 257–289.

Wessel, P., Smith, W.H.F., 1991. Free software helps map and display data. EOS Trans. AGU 72, 441, 445-446.

Wessel, P., Smith, W.H.F., 1995. New version of the generic mapping tools released. EOS Trans. AGU 76, 329.